

Supporting information

Chlorine tailored CdO_xCl_y/Al₂O₃ for syngas in electrochemical CO₂ reduction

Xin Wang,^a Zhen-Hong He,^{a,*} Hui-Hui Cao,^a Yu-Xuan Ji,^a Xuan-Lu Fan,^a Rui-Peng Yan,^a Kuan

Wang,^a Weitao Wang,^a Lu Li,^{c,d} Zhao-Tie Liu^{a,b,*}

^aShaanxi Key Laboratory of Chemical Additives for Industry, College of Chemistry and Chemical Engineering, Shaanxi University of Science and Technology, Xi'an 710021, China

^bSchool of Chemistry & Chemical Engineering, Shaanxi Normal University, Xi'an 710119, China

^cKey Laboratory of Auxiliary Chemistry and Technology for Chemical Industry, Ministry of Education, Shaanxi University of Science and Technology, Xi'an 710021, China

^dShaanxi Collaborative Innovation Center of Industrial Auxiliary Chemistry and Technology, Shaanxi University of Science and Technology, Xi'an 710021, China

*Corresponding authors: hezhenhong@sust.edu.cn (Zhen-Hong He); ztliu@snnu.edu.cn (Zhao-Tie Liu)

Materials

Aluminum nitrate ($\text{Al}(\text{NO}_3)_3 \cdot 9\text{H}_2\text{O}$, 99.0%, Shanghai Aladdin Biochemical Technology Co., LTD.), urea (99%, Shanghai Aladdin Biochemical Technology Co., LTD.), chromium chloride semi-pentahydrate ($\text{CrCl}_2 \cdot 5/2\text{H}_2\text{O}$, 99.0%, Shanghai Aladdin Biochemical Technology Co., LTD.), potassium bicarbonate (KHCO_3 , analytically pure, Tianjin Kemie Ou Chemical Reagent Co., LTD.), Toray carbon paper (CP, YLS-30T, $1\text{ cm} \times 1\text{ cm}$), and isopropyl alcohol (Analytically pure, Tianjin Kemie Ou Chemical Reagent Co., LTD.) are purchased from commercial sources. KSCN (>98.5%) was obtained from Greagent. Nafion perfluorinated resin, D520 (5 wt% in mixture of lower aliphatic alcohols and water) was provided by Shanghai Adamas Reagent Co., Ltd.

Electrochemical measurements

The electrochemical measurements were performed in an H-type cell by using a three-electrode system including working electrode, reference electrode (3 mol/L Ag/AgCl), and Pt mesh auxiliary electrode, respectively. The catalytic performances were evaluated on an electrochemical workstation (CHI660E, Shanghai Chenhua Co., Ltd). The working electrode was prepared by immobilization of the electrocatalyst on carbon paper ($1 \times 1\text{ cm}^2$). Typically, electrocatalyst (5 mg), isopropanol (600 μL), and Nafion solution (45 μL 5 wt%) were dispersed in the mixed under ultrasonication at room temperature for 30 min to obtain a uniform ink solution. Then, the catalyst ink (50 μL) was uniformly dripped onto a carbon paper ($1 \times 1\text{ cm}^2$) to act as the working electrode. The potentials reported are all converted into reversible hydrogen electrode (RHE) via the following equation.

$$E (\text{vs. RHE}) = E (\text{vs. Ag/AgCl}) + 0.197 + 0.059 \times \text{pH} \quad (1)$$

Before the test, the cathode cell was treated by Ar or CO_2 gas for 30 min, and then the LSV test

was carried out in the potential range from 0.62 ~ -1.38 V (vs. RHE) at a scanning rate of 50 mV·s⁻¹.

Ag/AgCl (3 M KCl) was used as the reference electrode.

The reaction gas was analyzed by GC (GC9790II, Zhejiang Fuli Analytical Instrument Co., Ltd), and the electrolyte after reaction was tested by ¹H NMR (Bruker Avance III 400 HD spectrometer).

Catalyst characterization

SEM images of the catalysts were recorded on SU8100.

TEM images of the catalysts were tested on FEI Tecnai G2 F20.

The XPS spectra were recorded on AXIS SUPRA using Al K α radiations. All the binding energies were calibrated with the C 1s line at 284.8 eV.

XRD patterns were conducted on a Rigaku D/max 2500 with nickel filtered Cu K α ($\lambda = 0.154$ nm) at 40 kV and 20 mA in the range from 5° to 80°.

N₂ adsorption/desorption and CO₂ adsorption experiments were tested on ASAP 2460 (Micromeritics, USA). Prior to the tests, 120 mg samples were degassed under vacuum of 10⁻⁵ torr at 150 °C for 12 h. The surface area of the samples was obtained according to Brunauer-Emmett-Teller (BET) method by analyzing the relative pressures (P/P₀) in the range from 0.05 to 0.3.

The Fourier-transform Infrared (FT-IR, Invenio) spectra were used to test the structural changes of functional groups of catalysts in the range of 500-4000 cm⁻¹.

Tables

Table S1 Summary of reported catalysts in electrocatalytic reduction of CO₂ to syngas

Entry	Catalyst	Electrolyte	E (vs. RHE) (V)	<i>j</i> (mA/cm ²)	Total FE values (%)	H ₂ /CO ratio	Ref.
1	Ag-P@HCS	0.5 M KHCO ₃	-0.7 ~ -1.1	-3 ~ -15	92 ~ 102	0.92 ~ 0.39	1
2	3D hp CuAg	0.1 M KHCO ₃	-0.6 ~ -1.0	-2 ~ -12	55 ~ 90	3:1 ~ 1:2	2
3	Te-Pd NP/C	0.1 M KHCO ₃	-0.6 ~ -1.0	-15 ~ -34	92 ~ 99	0.19 ~ 3.70	3
4	Br-Ag(OR)	2 M NH ₄ HCO ₃	-0.5 ~ -1.1	-5 ~ -110	100	0.30 ~ 3.35	4
5	R-Cu ₃ P/Cu	0.5 M NaHCO ₃	-0.21 ~ -1.10	-82.9 ~ -115	95 ~ 99	1:0.1 ~ 1:2.24	5
6	F-Cu ₂ O@ZIF-8	0.1 M KHCO ₃	-0.7 ~ -1.1	-2 ~ -14	75 ~ 95	2:1	6
7	CuFe ₂ @NG	1 M KHCO ₃	-0.51	-4.8	96	FE _{CO} 98%	7
8	4.3Pd-SnO ₂	0.5 M KHCO ₃	-0.5 ~ -1.1	-5 ~ -45	100	0.28 ~ 4.2	8
9	Fe-poN-C/Fe	0.5 M KHCO ₃	-0.24	-9	99	FE _{CO} : 99%	9
10	Fe _x C@CNT/N-MXene	0.1 M KCl	-0.8 ~ -1.2	15-34	95 ~ 104	0.22 ~ 2.82	10
11	1D/3D NPC-1000	0.5 M KHCO ₃	-0.35 ~ -0.75	7.5-12.5	38 ~ 98	0.20 ~ 1.28	11
12	Co-NHCS-400	0.5 M KHCO ₃	-0.6 ~ -1.1	-2 ~ -11	100	1.75 ~ 2.22	12
13	Cdhy-QS	0.5 M [Bmim]PF ₆ /MeCN	-2.3 ~ -2.6	-200	100	FE _{CO} : 100%	13
14	Cd/Cd(OH) ₂ /CP	[Bmim]PF ₆ -65wt%CH ₃ CN-5 wt%	-2.0(vs. Ag/Ag ⁺)	23.8	100	FE _{CO} : 98.3%	14
15	Cd-PCN-222HTs	[Bmim]PF ₆ (30 wt%)-H ₂ O (5wt%)-MeCN (65 wt%)	-2.0 ~ -2.4(vs. Ag/Ag ⁺)	68.0	100	FE _{CO} > 80%	15
16	CdO _x Cl _y /Al ₂ O ₃	0.5 M KHCO ₃	-1.0 ~ -1.4	5.8~59.0	96 ~ 108	0.3-3.1	This work
17	CdO _x Cl _y /Al ₂ O ₃	0.5 M KHCO ₃	-1.4	59.0	99	3.1	This work

Table S2. The analysis results of N₂ adsorption/desorption isotherms of samples

Catalysts	BET surface area (m²/g)	Pore size (nm)	Pore volume (cm³/g)
CdO _x Cl _y /Al ₂ O ₃ (1:1)	42	14.5	0.16
CdO _x Cl _y /Al ₂ O ₃ (2:1)	23	11.8	0.09
CdO _x Cl _y /Al ₂ O ₃ (3:1)	19	10.4	0.06
CdCl ₂	8	5.3	0.02
Al ₂ O ₃	574	3.6	0.48

Figures

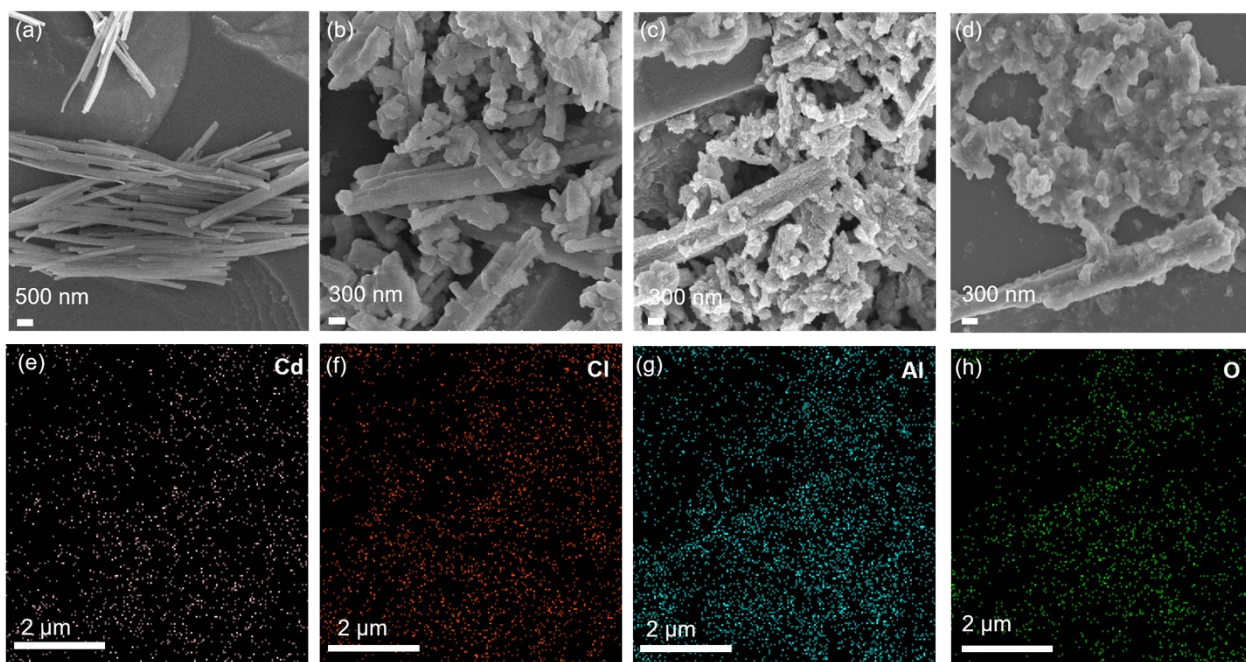


Fig. S1 SEM images of Al₂O₃ (a), CdO_xCl_y/Al₂O₃ (1:1) (b), CdO_xCl_y/Al₂O₃ (2:1) (c), CdO_xCl_y/Al₂O₃ (3:1) (d), and the EDS energy spectra of the CdO_xCl_y/Al₂O₃ (2:1) (e-h).

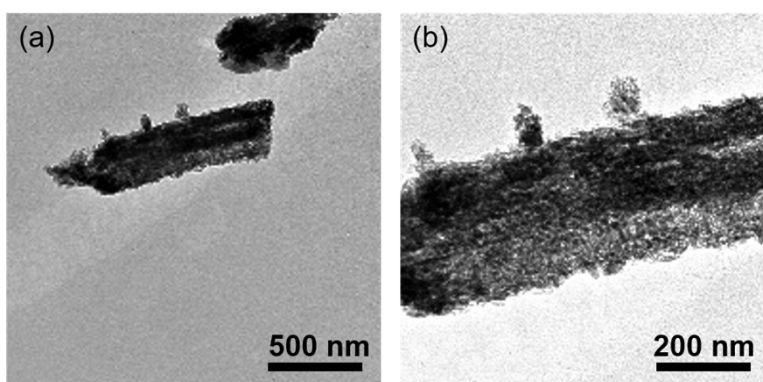


Fig. S2 TEM images of CdO_xCl_y/Al₂O₃ (2:1).

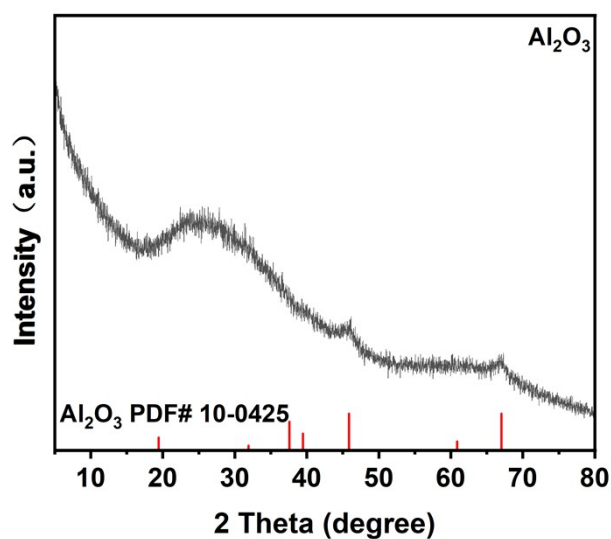


Fig. S3 XRD pattern of the Al_2O_3 .

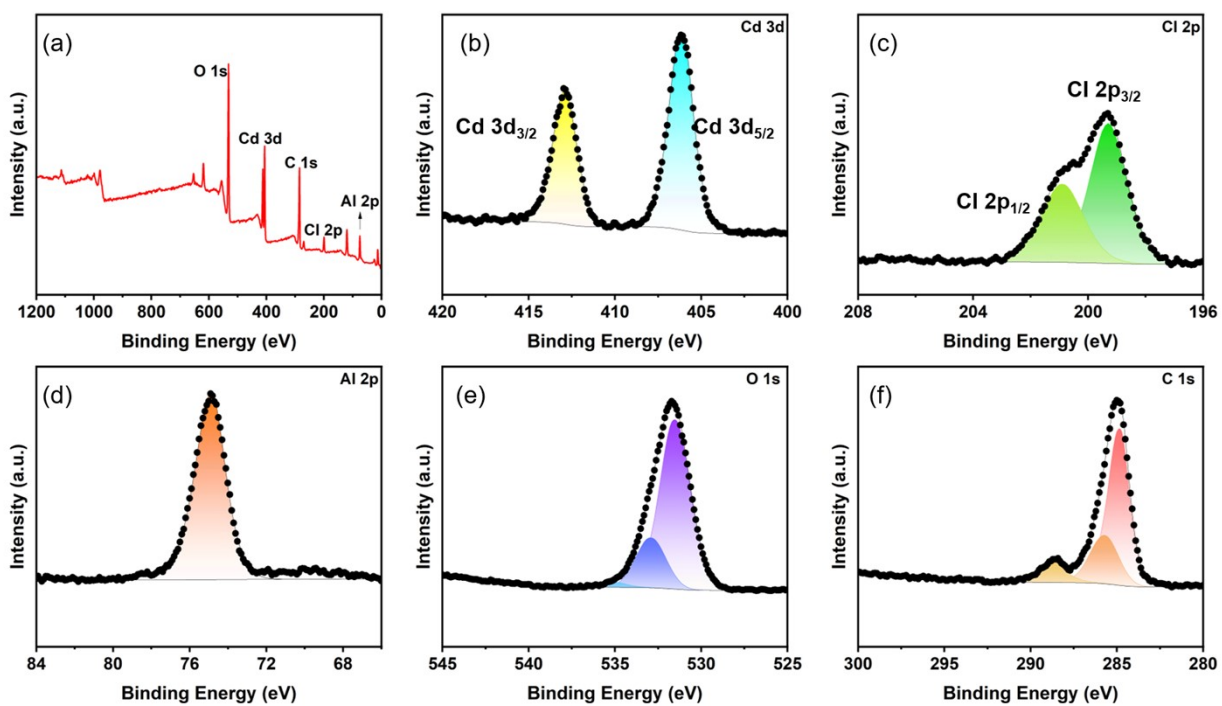


Fig. S4 XPS overall spectrum of the $\text{CdO}_x\text{Cl}_y/\text{Al}_2\text{O}_3$ (2:1) catalyst (a), Cd 3d (b), Cl 2p (c), Al 2p (d), O 1s (e), and C 1s (f) of the $\text{CdO}_x\text{Cl}_y/\text{Al}_2\text{O}_3$ (2:1).

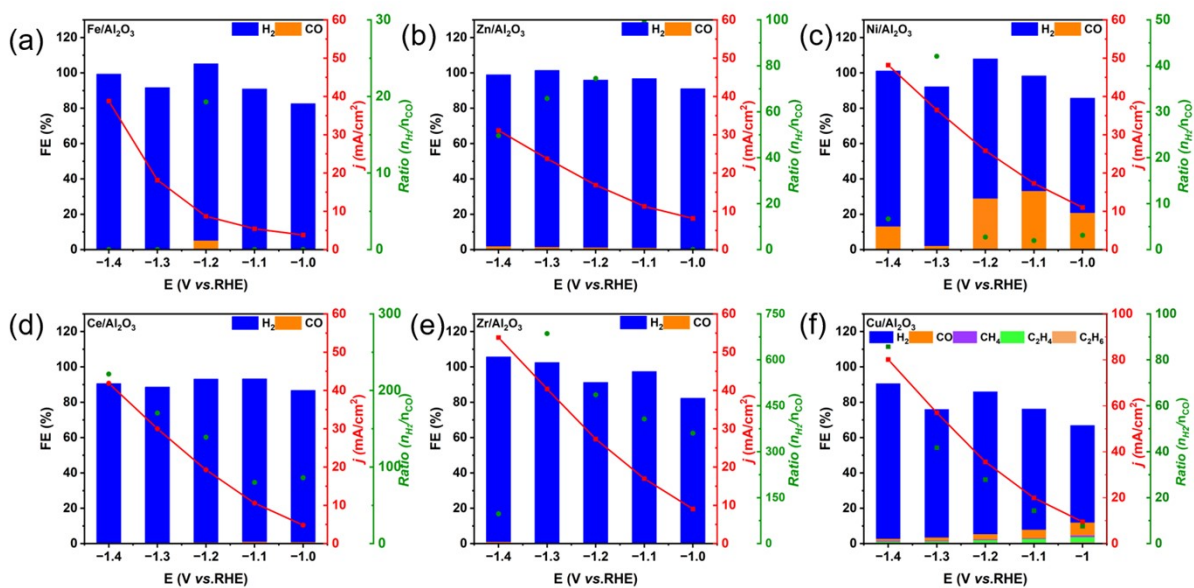


Fig. S5 Catalytic performances of the eCO₂RR over the Fe/Al₂O₃ (a), Zn/Al₂O₃ (b), Ni/Al₂O₃ (c), Ce/Al₂O₃ (d), Zr/Al₂O₃ (e) and Cu/Al₂O₃ catalyst (f).

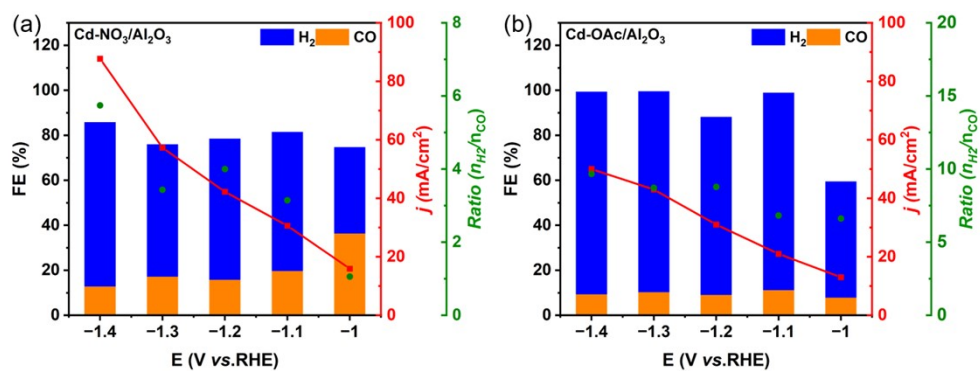


Fig. S6 Catalytic performances of the eCO₂RR over (a) the Cd-NO₃/Al₂O₃, (b) the Cd-OAc/Al₂O₃.

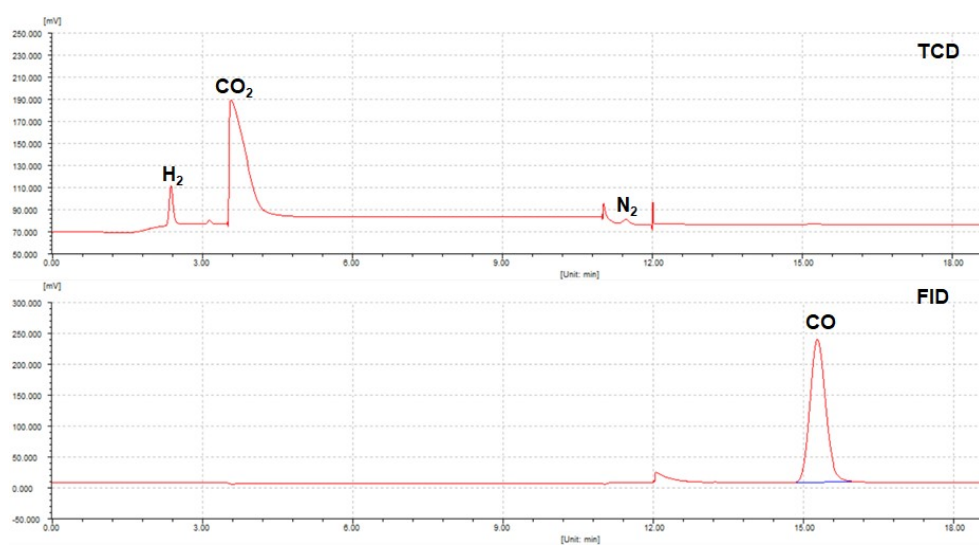


Fig. S7 GC data of eCO₂RR over the CdO_xCl_y/Al₂O₃ (2:1) catalyst.

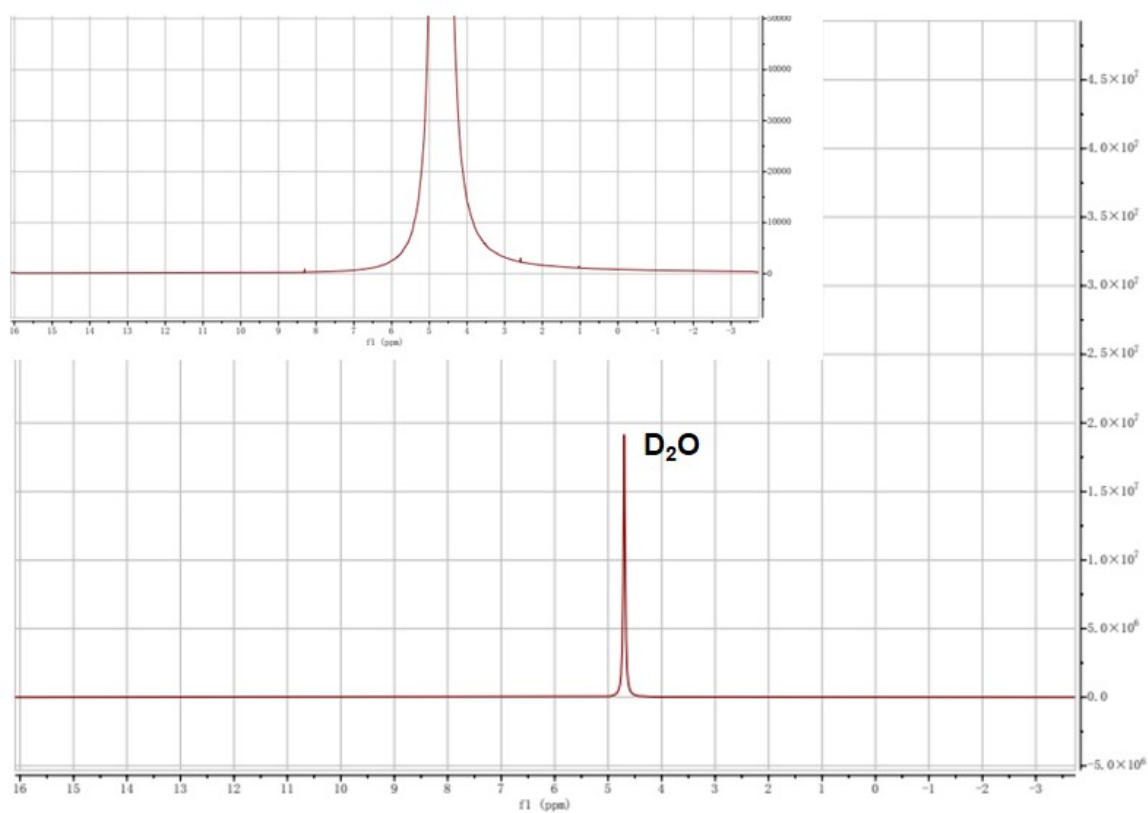


Fig. S8 ¹H-NMR spectrum of the electrolyte obtained from eCO₂RR over the CdO_xCl_y/Al₂O₃ (2:1) catalyst.

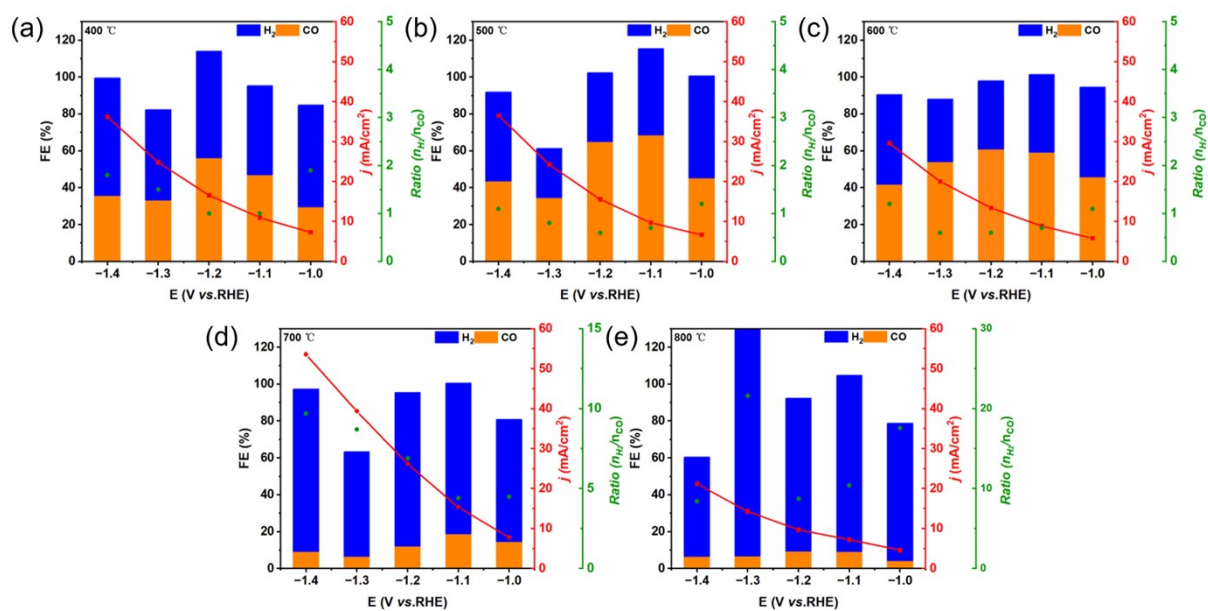


Fig. S9 The effect of temperatures in preparation of catalyst on the catalytic performances over the $\text{CdO}_x\text{Cl}_y/\text{Al}_2\text{O}_3$ (1:1).

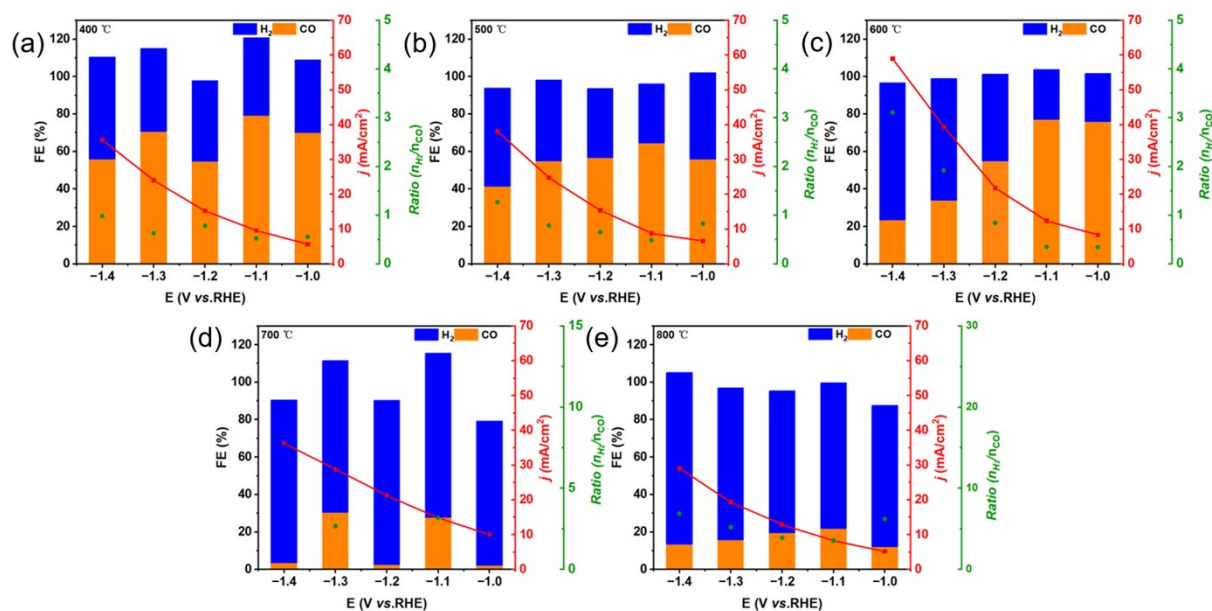


Fig. S10 Effect of preparation temperatures of catalyst on the catalytic performances over the $\text{CdO}_x\text{Cl}_y/\text{Al}_2\text{O}_3$ (2:1).

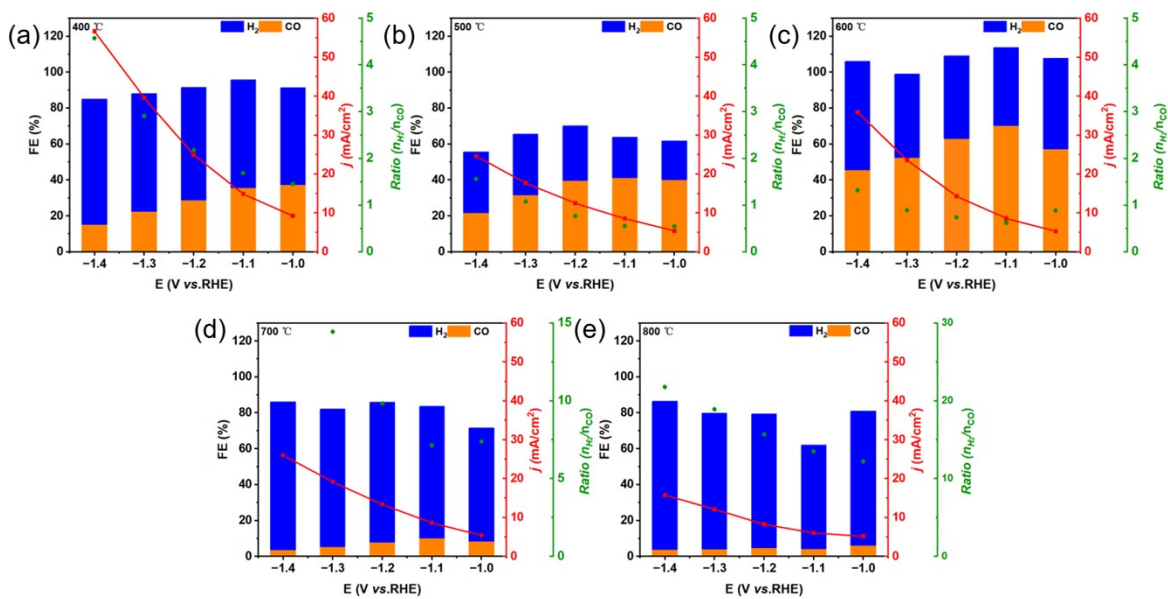


Fig. S11 Effect of preparation temperatures of catalyst on the catalytic performances over the CdO_xCl_y/Al_2O_3 (3:1) sample.

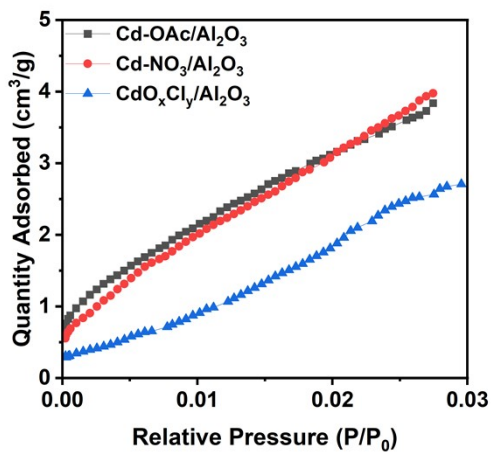


Fig. S12 CO₂ adsorption behaviors for diverse catalysts.

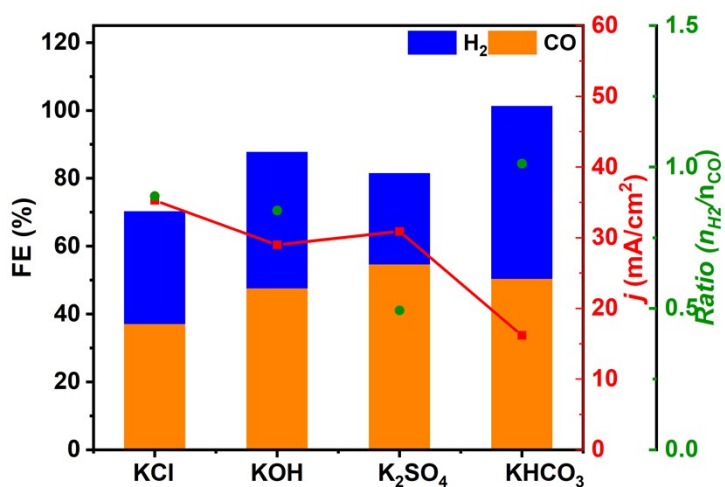


Fig. S13 Catalytic performances of eCO₂RR over the CdO_xCl_y/Al₂O₃ (2:1) catalyst in different electrolytes.

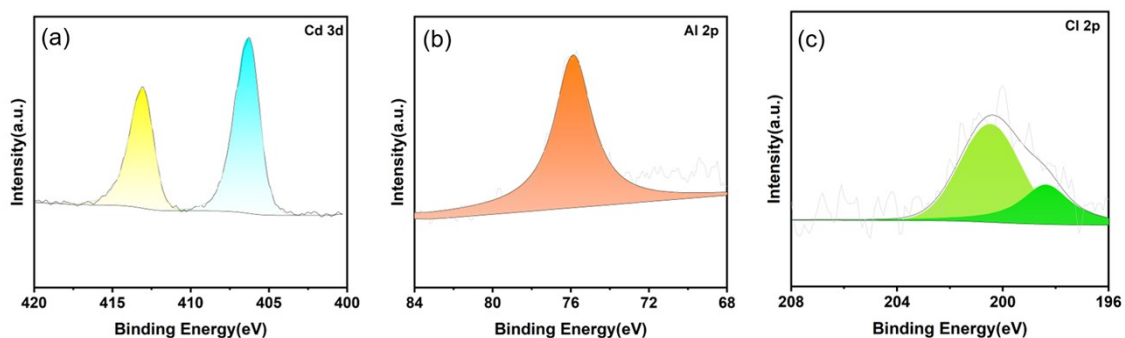


Fig. S14 XPS spectra of Cd 3d (a), Al 2p (b), and Cl 2p (c) of the used CdO_xCl_y/Al₂O₃ (2:1) catalyst.

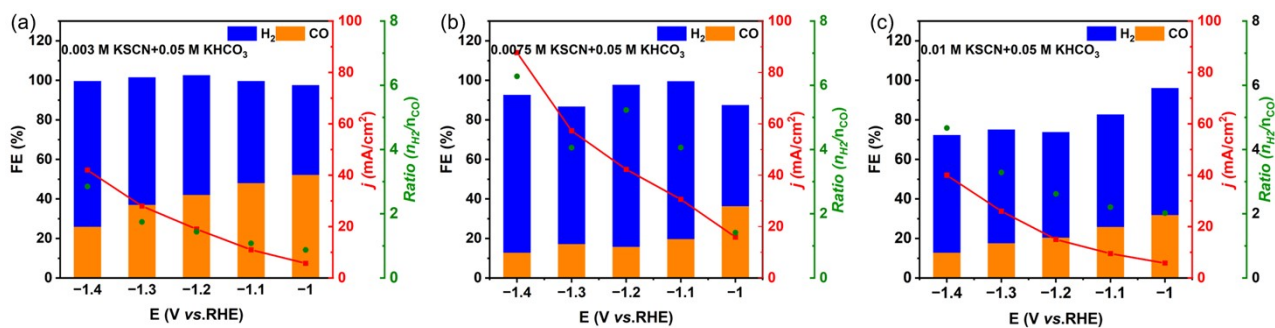


Fig. S15 Catalytic performances of eCO₂RR over CdO_xCl_y/Al₂O₃ poisoned by a (a) 0.003 M (b) 0.0075 M, (c) 0.01M KSCN solution. Other conditions were similar to those of **Fig. 6e**.

References

1. K. Li, Y. Kuwahara and H. Yamashita. *Appl. Catal. B-Environ.*, 2023, **331**, 122713.
2. W.-Y. Yan, C. Zhang and L. Liu. *ACS Appl. Mater. Interfaces*, 2021, **13**, 45385-45393.
3. K. Cao, Y. Ji, S. Bai, X. Huang, Y. Li and Q. Shao. *J. Mater. Chem. A*, 2021, **9**, 18349-18355.
4. H. Li, J. Gao, Q. Du, J. Shan, Y. Zhang, S. Wu and Z. Wang. *Energy*, 2021, **216**, 119250.
5. B. Chang, X.-G. Zhang, Z. Min, W. Lu, Z. Li, J. Qiu, H. Wang, J. Fan and J. Wang. *J. Mater. Chem. A*, 2021, **9**, 17876-17884.
6. H. Luo, B. Li, J.-G. Ma and P. Cheng. *Angew. Chem. Int. Ed.*, 2022, **61**, e202116736.
7. X. Du, L. Peng, J. Hu, Y. Peng, A. Primo, D. Li, J. Albero, C. Hu and H. García. *Nanoscale*, 2022, **14**, 11583-11589.
8. H. He, D. Xia, X. Yu, J. Wu, Y. Wang, L. Wang, L. Wu, J. Huang, N. Zhao, L. Deng and Y.-N. Liu. *Appl. Catal. B-Environ.*, 2022, **312**, 121392.
9. C. Wang, X. Wang, H. Ren, Y. Zhang, X. Zhou, J. Wang, Q. Guan, Y. Liu and W. Li. *Nat. Commun.*, 2023, **14**, 5108.
10. P.-P. Guo, Z.-H. He, H.-H. Cao, K. Wang, W. Wang, Y. Tian, J. Liu, L. Li and Z.-T. Liu. *Appl. Catal. B-Environ.*, 2024, **347**, 123786.
11. W. Zhang, H. Li, D. Feng, C. Wu, C. Sun, B. Jia, X. Liu and T. Ma. *Carbon Energy*, 2024, **6**, e461.
12. K. Li, Y. Kuwahara, K. Chida, T. Yoshii, H. Nishihara and H. Yamashita. *Chem. Eng. J.*, 2024, **488**, 150952.
13. C. Chen, X. Yan, R. Wu, Y. Wu, Q. Zhu, M. Hou, Z. Zhang, H. Fan, J. Ma, Y. Huang, J. Ma, X. Sun, L. Lin, S. Liu and B. Han. *Chem. Sci.*, 2021, **12**, 11914-11920.
14. X. Jia, K. Qi, J. Yang, Z. Fan, Z. Hua, X. Wan, Y. Zhao, Y. Mao and D. Yang. *Chem. Eng. J.*, 2023, **29**, e202302613.
15. J. Yang, J. Yu, W. Dong, D. Yang, Z. Hua, X. Wan, M. Wang, H. Li and S. Lu. *Small*, 2023, **19**, 2301319.